

## The Wake of Hurricane Allen in the Western Gulf of Mexico

DAVID A. BROOKS

*Department of Oceanography, Texas A&M University, College Station, TX 77843*

(Manuscript received 3 May 1982, in final form 21 September 1982)

### ABSTRACT

In August 1980, Hurricane Allen passed over a moored array of instruments recording current, temperature and conductivity in the western Gulf of Mexico. An alongshore surge occurred during the storm passage, with the horizontal current speed reaching  $91 \text{ cm s}^{-1}$  in the thermocline (200 m) and diminishing to  $15 \text{ cm s}^{-1}$  32 m above the bottom (732 m). A wake of near-inertial frequency internal waves commenced after the storm passed the array. The alongshore current oscillation reached a maximum range of  $50 \text{ cm s}^{-1}$  within 3 days and decayed thereafter with a time scale of about 5 days. The current oscillations were clockwise-polarized and slightly elliptical, with a period of 22–23 h or about 85% of the local inertial period. Near-uniform upwelling of  $\pm 20 \text{ m}$  occurred in the thermocline region (200–300 m) during the most intense part of the wake. Depth-leading phases of the horizontal current and temperature oscillations indicated downward radiation of wake energy. The wake oscillations were highly coherent over the vertical (500 m) and horizontal (100 km) scales of the array. The oscillations had a vertical scale much greater than the thermocline thickness ( $\sim 150 \text{ m}$ ) and several times the ocean depth at the array site. Because of the large vertical scale, downward radiation of wake kinetic energy was sufficient to account for the energy depletion rate in the thermocline, which suggests that dissipation was relatively unimportant during the early stage of wake decay.

### 1. Introduction and setting

Observations of the oceanic response to a hurricane usually exist as fortuitous "events" in data sets collected for other reasons. In the western Gulf of Mexico, for example, Franceschini and El-Sayed (1968) modified their cruise track to give before-and-after hydrographic surveys in the path of Hurricane Inez. In the northwestern Gulf, the shallow ocean current response to the fringe of Hurricane Anita was reported by Smith (1978), and Forristall *et al.* (1977) described the current response to Hurricane Delia as the storm passed over a drilling platform on the Texas shelf. The currents were measured in water depths of about 20 m, and the observed responses were found to be frictionally dominated. In the present case, Hurricane Allen passed over an array of 10 Aanderaa current meters and a 100 m thermistor string, which were deployed on three moorings over the 730 m isobath in the western Gulf (Fig. 1). The moorings were spaced about 55 km apart, in a vertical plane approximately perpendicular to the track of the approaching storm. The eye of the hurricane passed within  $\sim 60 \text{ km}$  of the southern mooring. The instruments spanned the depth range of 200–700 m, which included most of the thermocline. The mid-thermocline (200–300 m) response was dominated by a wake of near-inertial frequency internal waves, which is described here.

After deploying the moorings, a hydrographic survey was conducted in the western Gulf (Brooks and

Eblé, 1982). The survey was completed about two weeks before the hurricane passed through the area. With some XBT data from a nearly simultaneous cruise,<sup>1</sup> the  $14^\circ\text{C}$  isothermal surface depth was contoured and is shown in Fig. 1. The closed depth contours and the prominent depression of the  $14^\circ\text{C}$  surface centered near  $95^\circ\text{W}$ ,  $24.5^\circ\text{N}$  indicate an anticyclonic circulation, which is a persistent feature in the western Gulf (cf. Nowlin, 1972; Merrell and Morrison, 1981; Brooks and Legeckis, 1982).

The central mooring included a thermistor string with 10 m vertical resolution in the depth range 200–300 m. Temperature and density profiles from representative stations in the northern flank (B4) and in the center (B14) of the anticyclone are shown in Fig. 2. The current meters spanned the lower two-thirds of the main thermocline, as judged by the temperature profile at station B4.

The instruments recorded data from 18 July 1980 to 4 February 1981. The current meters at the 200 and 450 m depths on the northern mooring (N) lost their rotors just after and just before the hurricane passed on 9 August, respectively, but they provided full-length records of temperature, conductivity and current direction. The basic sampling interval was 0.5 h for the current meters and 1.0 h for the thermistor recorder. After editing and calibration, the data were

<sup>1</sup> R/V *Longhorn* data were provided by Dr. A. Sturges of the Florida State University.

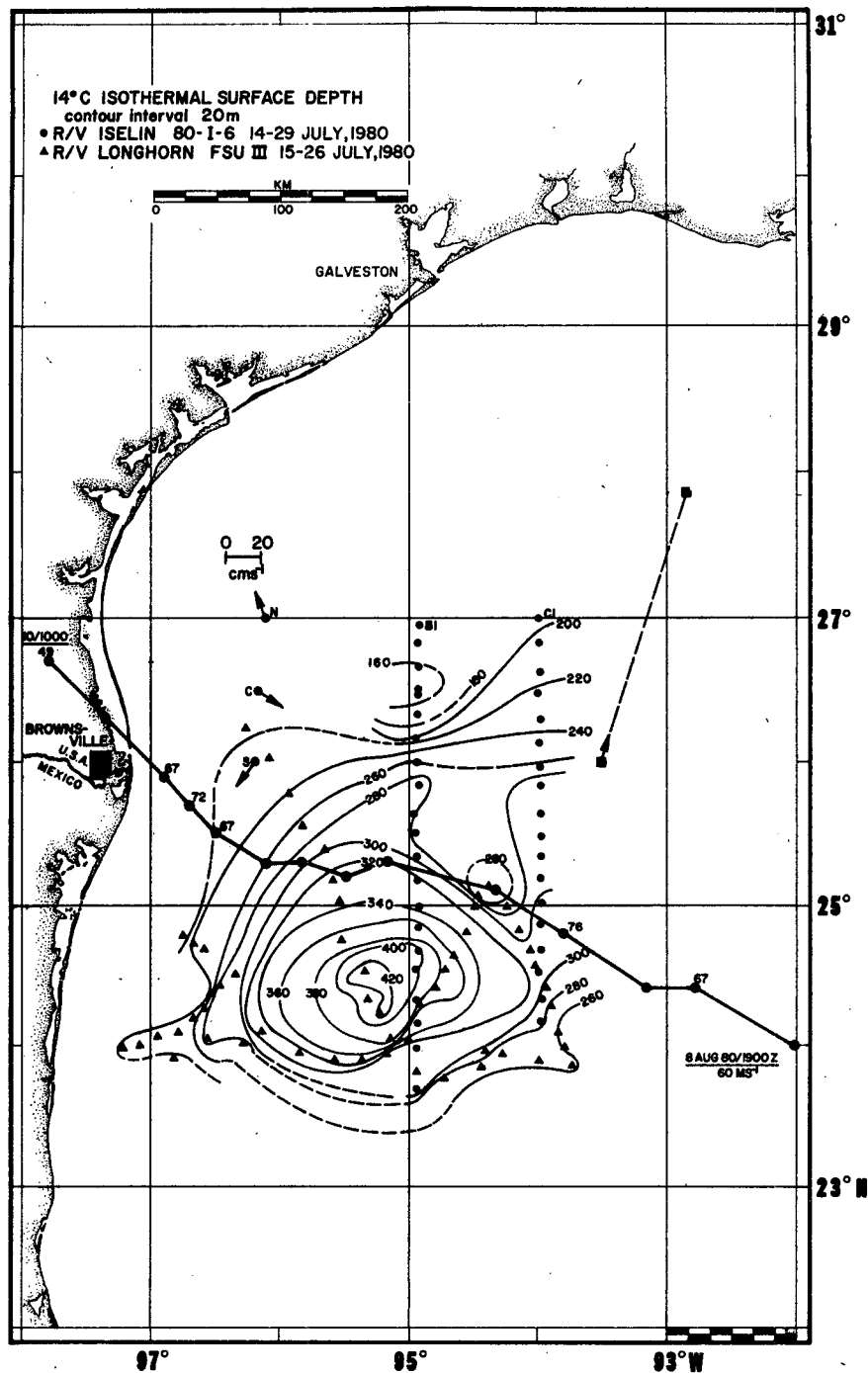


FIG. 1. Map of western Gulf of Mexico, showing ship stations (dots and triangles), depth contours (m) of the 14°C surface depth, the westward track of Hurricane Allen (solid circles), and the location of the north (N), central (C), and south (S) instrument moorings. Three-hourly positions of the hurricane are shown by the dots on the trackline, starting at 1900 GMT 8 August 1980. The maximum surface wind speed ( $\text{m s}^{-1}$ ) is shown adjacent to the dots, when it changed from the value at the previous position. Current vectors at the 200 m depth on the day prior to the storm's passage are shown at the mooring locations. The initial (9 August) and final (12 August) positions of NDBO buoy 42002, which parted its mooring cable during the storm, are shown by the solid squares.

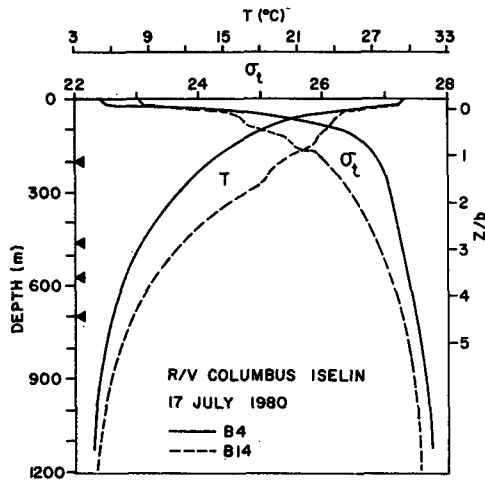


FIG. 2. Temperature and  $\sigma_t$  versus depth at a station from the northern edge of the anticyclone (B4) and one in the center of the anticyclone (B14). The depth scale on the right margin is normalized by the thermocline thickness scale at station B4,  $b = 150$  m. The depths of the current meters on the central mooring are shown by the arrowheads. The pre-storm surface mixed layer was 30–50 m deep.

filtered with a 3 h low-pass (3 HRLP) filter, which attenuates sampling noise and other short-period fluctuations. A 40 h low-pass (40 HRLP) filter was then applied to separate the tidal, inertial and other fluctuations with 3–40 h periods from fluctuations with periods > 40 h. Band-passed records were obtained by subtracting the 40 HRLP records from the 3 HRLP records.

**2. Hurricane Allen**

Hurricane Allen was the strongest storm ever recorded in the Caribbean (Woodley *et al.*, 1981). As

the storm was entering the Gulf, a NOAA aircraft survey located the maximum flight level wind speed of  $78 \text{ m s}^{-1}$  about 40 km to the right of the storm's direction of advance (Jones *et al.*, 1981). These were the highest wind speeds ever measured by a hurricane reconnaissance aircraft. An aircraft survey performed on 9 August, as the storm passed over the mooring array, showed flight-level maximum winds of about  $50 \text{ m s}^{-1}$  located 20 and 80 km to the right of the storm track (P. Black, personal communication, and see Fig. 3). The outer wind speed maximum passed midway between the southern and central moorings.

The storm track crossed the anticyclone north of its central depression (Fig. 1). Between  $93$  and  $95^\circ\text{W}$ , the storm's translation speed was steady at about  $7 \text{ m s}^{-1}$  toward the WNW. After crossing  $95^\circ\text{W}$ , nearest the center of the anticyclone, the translation speed slowed to about  $3.5 \text{ m s}^{-1}$  toward the west. As the storm passed the western side of the anticyclone and approached the coast, the maximum winds decreased rapidly. The storm then veered toward the northwest on a track which brought the highest winds within 50–75 km north of Brownsville, Texas. The maximum measured wind speed at Brownsville was  $22 \text{ m s}^{-1}$  and the lowest pressure was 970 mb.

The oceanic response to the hurricane winds was dramatic. The most energetic response occurred at the uppermost (200 m) instrument on the  $C_1$  mooring, from which the data are shown in Fig. 4 for the 29-day period centered on the day of the storm's passage (9 August). The initial response at  $C_1$ , which is typical in form of that at the other instruments, consisted of a rapidly-accelerated southward surge reaching  $91 \text{ cm s}^{-1}$ , accompanied by equally rapid temperature and salinity increases. The surge diminished shortly after the hurricane eye's closest approach to the mooring at 0000 GMT on 10 August, and a wake

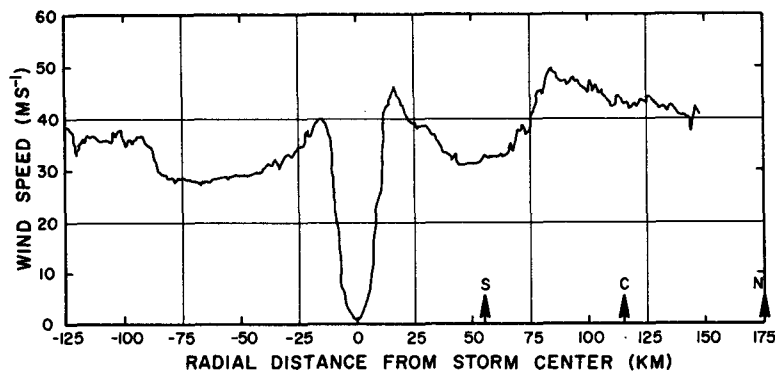


FIG. 3. Wind speed along a south-to-north flight path at 3 km height on 9 August 1980 (from P. Black, NOAA, personal communication). The aircraft survey was made along  $96^\circ 20' \text{W}$ , just after the storm passed the longitude of the moored array. The double wind speed maximum was associated with the unusual radial cloud and precipitation structure of Hurricane Allen (cf. Jones *et al.*, 1981). The approximate locations of the current meter moorings are shown by the vertical arrows.

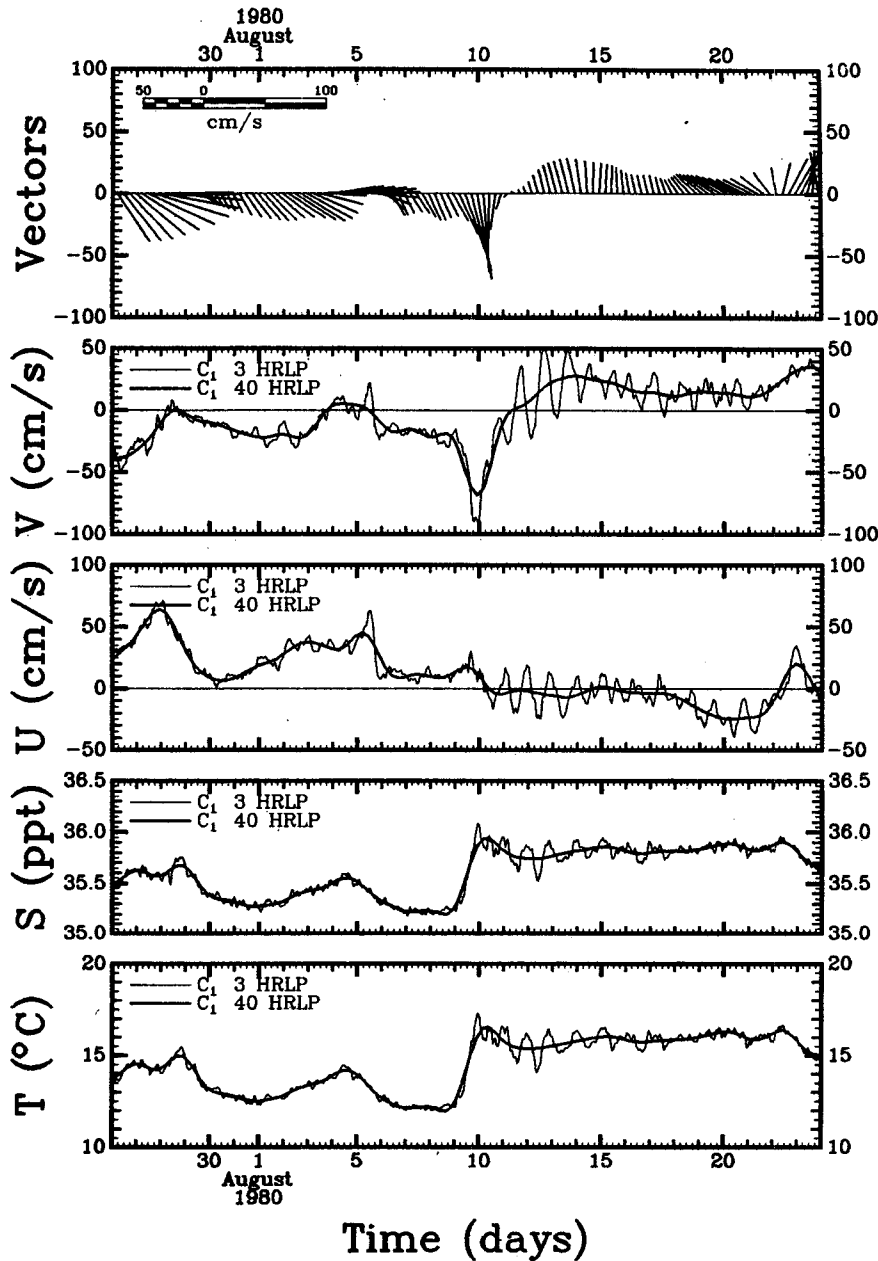


FIG. 4. Velocity vectors, northward ( $v$ ) and eastward ( $u$ ) velocity components, salinity, and temperature records from the central mooring 200 m depth, for a 29-day period centered on the time of Hurricane Allen's passage over the array. The storm's closest approach to the central mooring occurred at  $\sim 0000$  GMT 10 August. The heavy lines and vectors are low-pass filtered to remove fluctuations with periods  $\leq 40$  h. Vectors pointing "up" indicate northward flow.

oscillation having a near-inertial period began just as the storm passed, with the longshore current range reaching  $\sim 50 \text{ cm s}^{-1}$  several days later. Subsequently, the wake decayed with a time scale of about 5 days. The low-frequency (40 HRLP) current reversed from essentially southward before the storm to northward after it. The northward currents and the relatively

high temperature and salinity persisted for several weeks after the storm passed. First-order statistics of the current and temperature fluctuations during the 29-day period are shown in Table 1. For further analysis, tidal motions were extracted from the 29-day current records by subtracting a four-constituent tide determined by a simultaneous least-squares tech-

nique. The  $O_1$  constituent had the largest amplitude ( $\sim 4 \text{ cm s}^{-1}$ ), which accounted for  $\sim 10\%$  of the variance at the 200 m depth.

**3. The surge response (9 August)**

The temperature, salinity and southward current increases at  $C_1$  began about 0000 GMT 9 August, when the storm's center was  $\sim 380 \text{ km}$  distant (Figs. 1 and 4). At that time, the winds in the array area were generally  $10\text{--}20 \text{ m s}^{-1}$  from the northeast, so the surface waters were subjected to a wind stress toward the west and south by the outer storm winds.

The southward current speed at  $C_1$  increased from 20 to  $91 \text{ cm s}^{-1}$  and the temperature and salinity increased by about  $5^\circ\text{C}$  and  $0.9\text{‰}$  between 9 and 10 August (Fig. 4). Similarly rapid but smaller-amplitude increases occurred at the other instruments. The maximum values occurred within 1 h of the time of the eye's closest approach to the southern mooring (0000 GMT 10 August). After passage of the eye, the wind rapidly shifted to SE and then S. The southward current then relaxed, and within 2 days it overshot

TABLE 1. First-order statistics of the 3 h low-pass filtered current component and temperature records, for the 29-day period 26 July–24 August 1980, Hurricane Allen.  $T$  ( $^\circ\text{C}$ );  $u, v$  ( $\text{cm s}^{-1}$ ).

		Minimum	Maximum	Mean	Standard deviation
$N_1$	$T$	14.62	17.16	15.62	0.51
$N_2$	$T$	9.35	11.77	10.32	0.39
$N_3$	$u$	-11.67	11.13	0.18	3.67
	$v$	-15.19	9.19	-2.15	4.97
	$T$	5.42	6.49	5.88	0.24
$C_1$	$u$	-39.12	71.12	10.71	22.15
	$v$	-91.19	52.01	-1.89	24.31
	$T$	11.99	17.29	14.57	1.47
$C_2$	$u$	-18.45	37.89	7.85	10.00
	$v$	-47.22	23.09	-6.02	10.78
	$T$	8.74	10.52	9.61	0.40
$C_3$	$u$	-12.01	18.88	2.65	5.76
	$v$	-26.17	26.93	-2.29	10.57
	$T$	7.92	9.52	8.62	0.39
$C_4$	$u$	-23.08	14.17	0.84	5.55
	$v$	-15.04	17.19	-2.09	5.25
	$T$	6.28	7.98	7.05	0.26
$S_1$	$u$	-37.51	40.50	-1.12	13.11
	$v$	-52.93	35.25	2.06	15.80
	$T$	12.24	15.43	13.90	0.70
$S_2$	$u$	-19.17	32.51	0.19	7.66
	$v$	-39.07	36.46	1.01	10.70
	$T$	8.26	10.18	9.37	0.32
$S_3$	$u$	-15.65	25.65	6.41	8.34
	$v$	-22.29	16.40	-3.22	5.68
	$T$	6.23	7.79	6.99	0.35

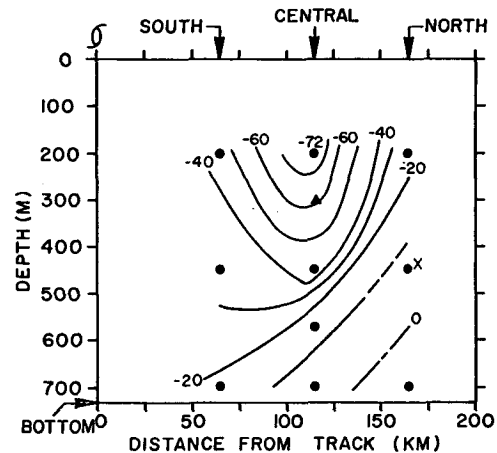


FIG. 5a. Contours of the difference between the maximum  $v$ -component at each instrument on 10 August 1980 and the corresponding mean value on 8–9 August ( $\text{cm s}^{-1}$ ). The contoured field is the hurricane-induced velocity change which occurred during that period. Southward velocities are negative.

its pre-storm condition and reversed to northward. Superimposed on this transient surge was a growing oscillatory wake, which is evident in the 3 HRLP data of Fig. 4. The surge magnitude, calculated for each instrument as the maximum  $v$ -component amplitude on 10 August minus the 8–9 August mean 3 HRLP  $v$ -component, is contoured in Fig. 5a, showing the storm-induced change of the longshore currents that occurred in about 24 h. The strongest surge occurred at the central mooring. The surge may have been augmented by the proximity of the continental margin, which has a locally steep slope near the central mooring location (Fig. 5b).

Before the storm passed, relatively cool and fresh water was moving offshore at the central mooring 200

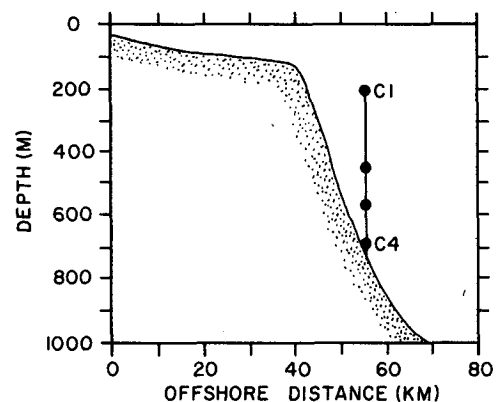


FIG. 5b. Depth profile of the continental shelf and slope at the latitude of the central (C) mooring, which supported current meters  $C_1\text{--}C_4$  at the indicated depths. The top current meter ( $C_1$ ) was about 50 m deeper than the shelf "break," which was located about 12 km west of the mooring.

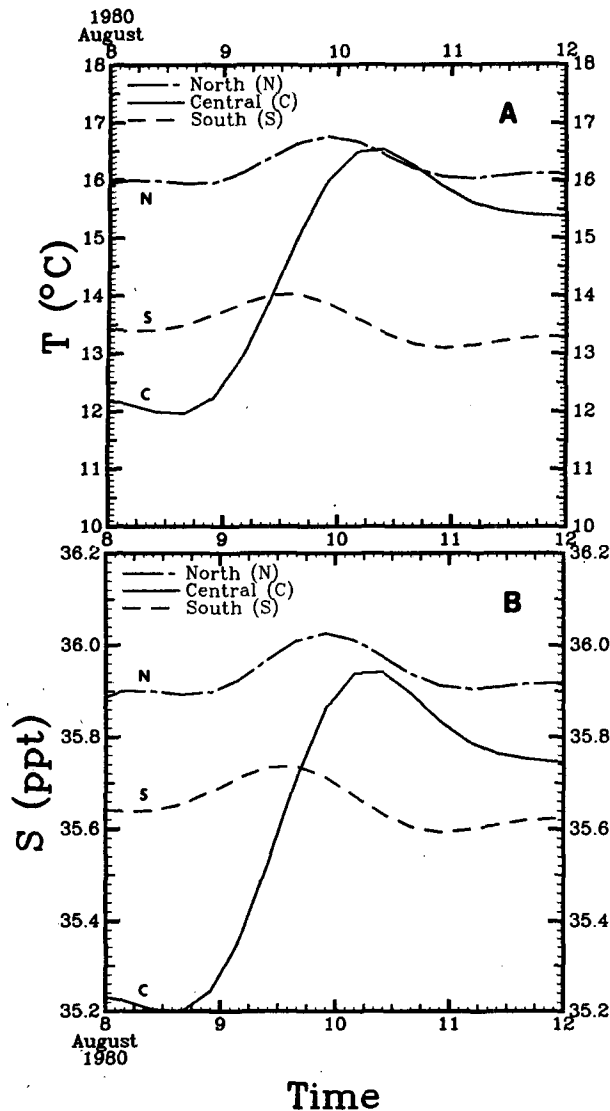


FIG. 6. The initial temperature (A) and salinity (B) response to Hurricane Allen at the 200 m depth on the three moorings (N, north; C, central; S, south). The data shown have been 40 h low-pass filtered.

m depth (Figs. 1 and 6). The cool, fresh water was bounded on the northern and southern sides by substantially warmer and saltier water, which was moving slowly onshore at the northern mooring. During the July 1980 cruise, the mid-thermocline water at the central mooring was fresher than any other water shallower than about 400 m, which suggests the offshore influence of Texas shelf water. Outbreaks of Texas coastal water have often been observed near 26°N (e.g., Nowlin, 1972; Brooks and Legeckis, 1982).

Between 9 and 10 August, during the maximum storm winds, the temperature and salinity at the central mooring increased to almost their pre-storm val-

ues at the northern mooring (Fig. 6). The most direct explanation is that, under the strong northeast storm winds, the interleaved band of cool, fresh mid-thermocline water was obliterated by mixing with the southward-moving, warm, salty water from the north. Vigorous mixing at the 200 m depth is indicated, as there is little evidence (in Fig. 6) of cooling or freshening at the southern mooring, as one would expect were simple southward advection of the existing  $T$ - $S$  structure the sole explanation. It is not clear if the mixing energy penetrated from the shallow ( $\sim 30$  m) pre-storm surface mixed layer, or if it was locally extracted from the jet-like surge that was most intense at the central mooring (Fig. 5). Franceschini and El-Sayed (1968) also found several-degree temperature increases at the 200 m depth after Hurricane Inez, which was a storm of lesser magnitude than Allen.

#### 4. The wake response (10–16 August)

The storm wake persisted for about a week after a several-day growth period. The band-pass filtered data from the  $C_1$  instrument are shown in Fig. 7 for the active wake period. The amplitude of the first oscillation is exaggerated by the 40 HRLP filter response.

A purely inertial wake would have clockwise-polarized, circular particle motions confined to horizontal planes. The Hurricane Allen wake oscillation had a maximum period of 23 h, or about 85% of the inertial period (IP) at the central mooring. After a short interval ( $\sim 1$  day) of rectilinear motions, the horizontal velocity oscillations became clockwise-polarized, but with elliptical particle motions (Fig. 7). During the time of the maximum wake amplitude (11–12 August), the ellipticity of the velocity hodograph at  $C_1$  was  $\sim 1.4$ , which can be compared with an expected ellipticity of 1.2 for a wake period of 0.85 IP (cf. Phillips, 1969). The temperature and salinity fluctuations were highly correlated with the velocity fluctuations and they were in-phase with the  $u$  component.

Within several days after the storm passed, the kinetic energy of the wake penetrated the thermocline (Fig. 8). The amplitude of the velocity oscillations decreased with depth, but a phase difference across the thermocline soon developed, with the deeper oscillations leading the shallower ones. By the time of the maximum wake amplitude, the phase lead at the 575 m depth had increased to 9 h, relative to the 200 m depth. A similar deep phase lead occurred at the southern mooring, although the velocity-component amplitudes were about a factor of 2 smaller there.

The 9 h phase difference indicates that the wake had a vertical scale of  $\sim 1$  km in the thermocline, which is much greater than the thermocline thickness scale (150 m) and greater than the ocean depth at the

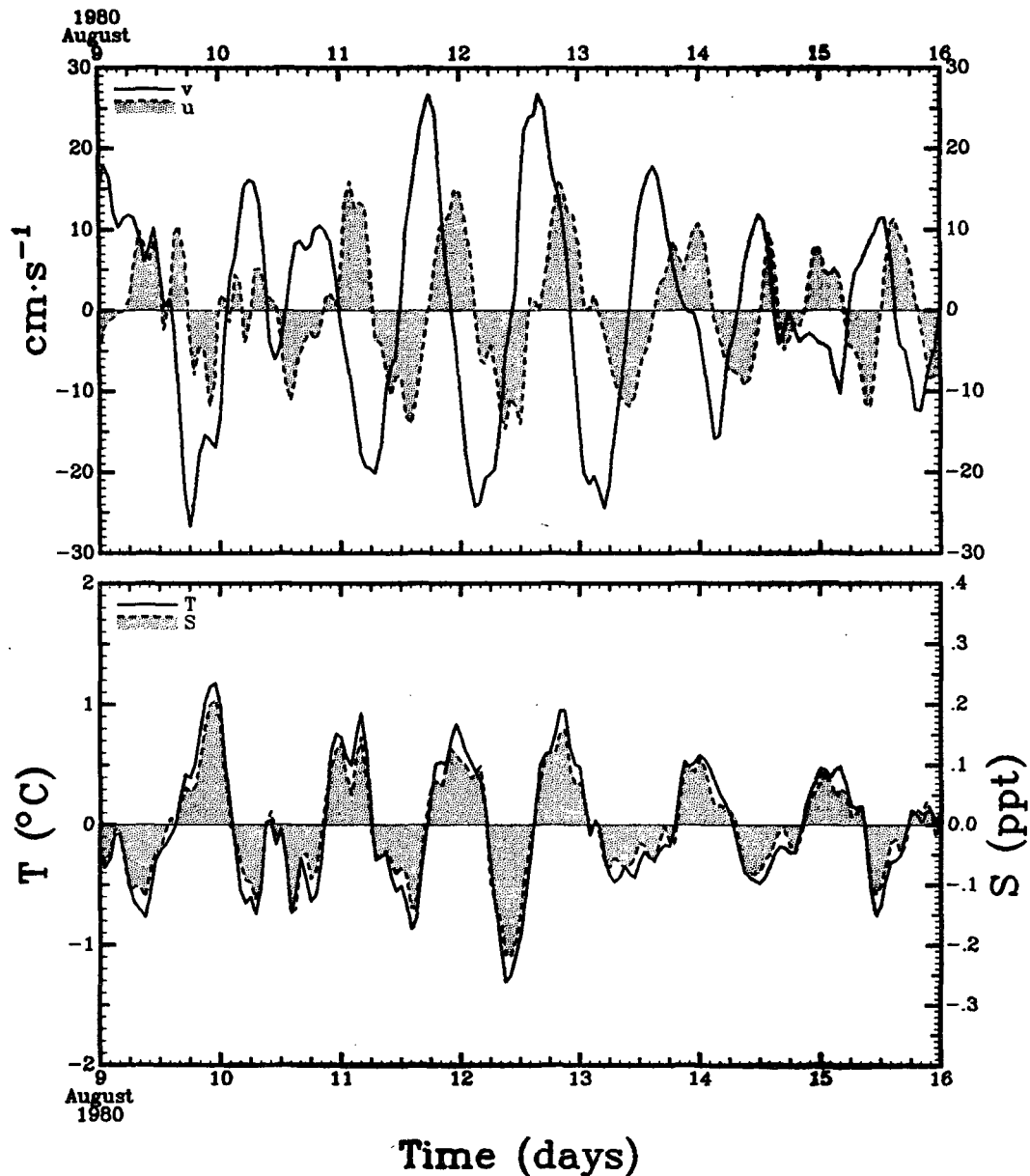


FIG. 7. Northward ( $v$ ) and eastward ( $u$ ) velocity components and temperature ( $T$ ) and salinity ( $S$ ) bandpass-filtered wake oscillations at the 200 m depth on the central mooring ( $C_1$ ). The clockwise, elliptical polarization expected for near-inertial oscillations is evident. The temperature record indicates upwelling displacements of  $\sim 20$  m in the mid-thermocline.

array location (730 m). During the early part of the wake, the thermocline phase difference was very small, and the indicated vertical scale of the storm response in the thermocline was  $\gg 1$  km.

The relative phase of the  $v$  component at the central mooring is contoured in Fig. 9. The phase lead increases with depth, relative to the 200 m depth, in the shaded areas. The figure shows a regular build-up of the deep phase lead as a function of depth and time until about 4 IP after the passage of the storm,

when a mid-thermocline phase minimum developed. The leading phases at depth are consistent with downward propagation of energy through the thermocline, which can be simply illustrated by elementary inertial-internal wave theory with a constant Brünt-Väisälä frequency  $N$  (e.g., Phillips, 1969). Except for the shallow surface mixed layer, such a simplification may be reasonable for the pre-storm density profile (Fig. 2). Deepening of the mixed layer by the storm winds increases the likely importance of higher in-

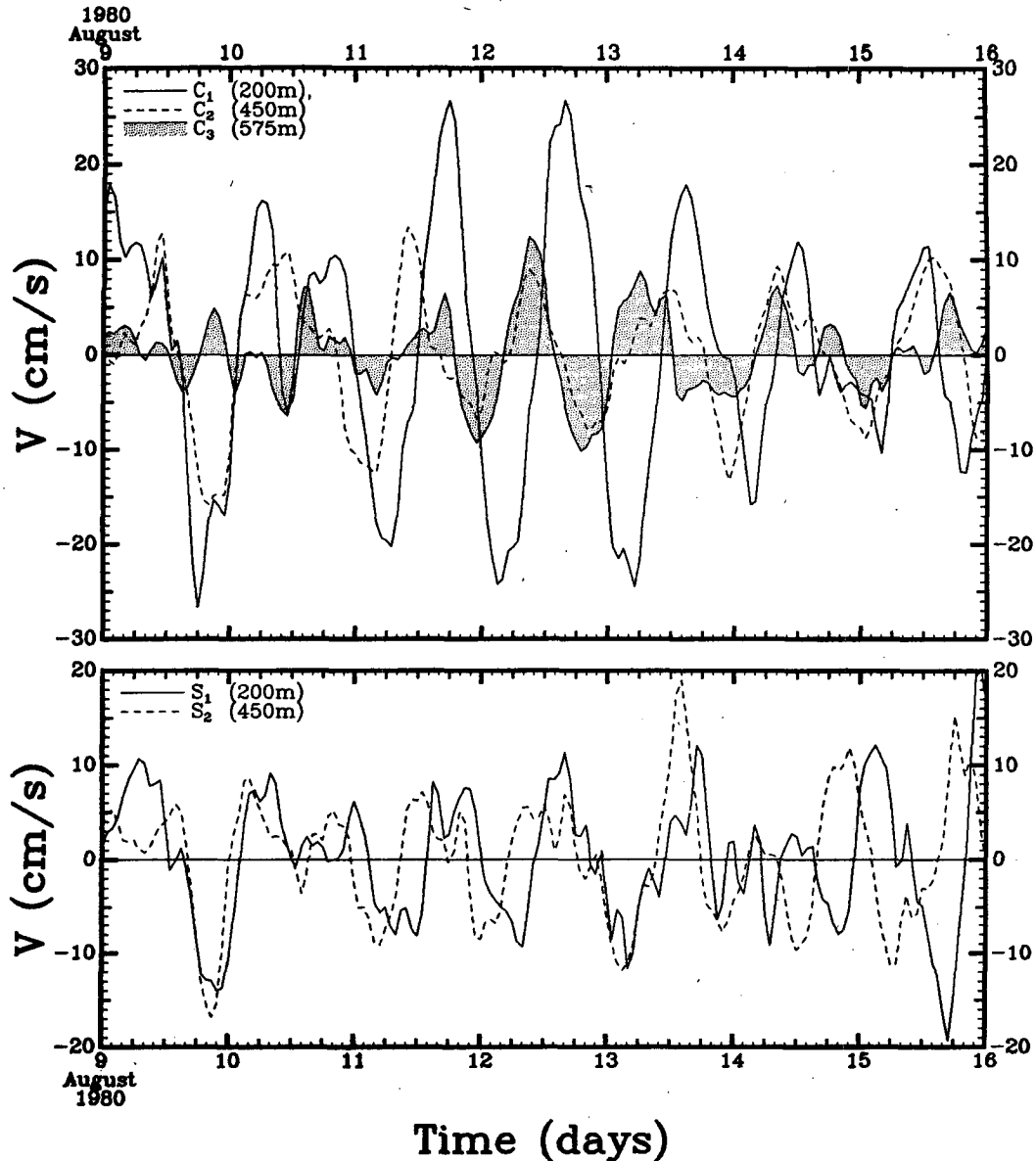


FIG. 8. The vertical structure of the northward ( $v$ ) wake velocity component at the central (C) and southern (S) moorings. The data have been 3–40 h band-pass filtered to separate the wake oscillations from other motions, which exaggerates the amplitude of the first few oscillations after 9 August. The depth-leading phases are an indication of downward energy flux in the thermocline.

ternal modes. In view of the large vertical scales already mentioned, however, it appears that the gravest (free-surface) internal mode was significant in the wake structure.

For  $N^2$  constant, the energy transport velocity vector,  $C_g = (C_{gy}, C_{gz})$ , can be determined in terms of the phase velocity vector  $C_p = (\omega l^{-1}, \omega m^{-1})$  as

$$C_{gy} = \omega l^{-1} (N \omega^{-1} \tan \theta)^2, \quad (1a)$$

$$C_{gz} = -\omega m^{-1} (N \omega^{-1} \tan \theta)^2, \quad (1b)$$

where  $L_y \gg L_z$  has been used. It may be verified from the phase differences between the central and southern moorings that the horizontal scale  $L_y \approx 370 \text{ km} \gg L_z \approx 1 \text{ km}$  during the maximum wake response (Fig. 8). The coordinate system has been chosen such that the hurricane travelled in the negative  $x$ -direction, and such that  $(y, z)$  are positive in the (northward, upward) direction. The wake frequency is  $\omega$ , and  $\tan \theta = lm^{-1}$  gives the angle  $\theta$  between phase vector and the vertical, where the wavenumbers  $(l, m) = 2\pi(L_y^{-1}, L_z^{-1})$ . Using the length scales determined



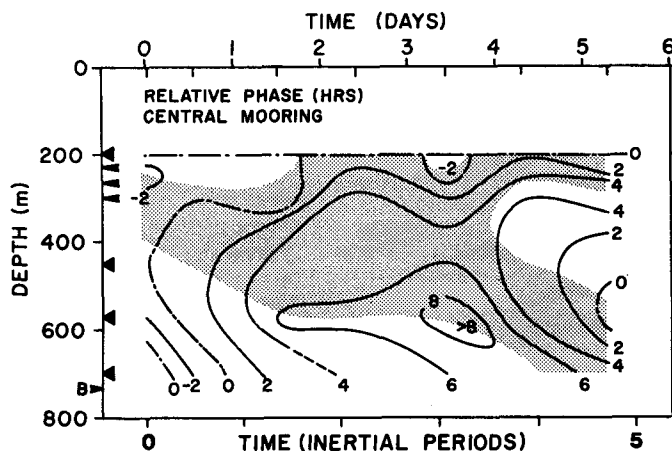


FIG. 9. Contours of vertical phase of the wake *v*-component oscillations at the central mooring, relative to the 200 m depth. The phase lead increases with depth in the shaded region. Relative times of *v*-component velocity maxima at the *C*<sub>1</sub> instrument are shown by the tick marks on the lower side of the upper axis. The inertial period scale applies to the central mooring latitude (26°30'N). The phase values were obtained from the 3–40 h band-passed current meter *v*-component records (at depths shown by the large arrowheads) and from several thermistors (at depths shown by the slender arrowheads).

from Fig. 8,  $\tan\theta = 0.27 \times 10^{-2}$  which can be compared with  $\tan\theta = N^{-1}(\omega^2 - f^2)^{1/2} = 0.43 \times 10^{-2}$ , calculated directly from the dispersion relation with  $\omega = 1.2f$  and with *f* the Coriolis parameter.

From (1b), the kinetic energy propagates vertically with the opposite sense of the phase propagation. Thus, the depth-leading phases of the wake clearly indicate downward propagation of energy in the thermocline. This is a consequence of outward radiation of energy from the surface layer which, by (1), requires that the phase vector be tipped slightly out of the vertical.

A density change across the thermocline of  $2\sigma_t$  units in 375 m leads to  $C_{gz} \approx 60 \text{ m day}^{-1}$  during the most energetic part of the wake response. Because of its cubic dependence on  $L_z$ ,  $C_{gz}$  is very sensitive to the vertical scale estimate. Pollard (1980) calculated the vertical group velocity at Site D to be 0.03 to 3  $\text{m day}^{-1}$ , leading to the conclusion that the vertical energy flux due to inertial-internal wave radiation was insufficient to account for the observed depletion of surface mixed layer kinetic energy. In the present case, the absence of observations in the surface mixed layer precludes an analogous calculation. However, the energy flux (*F*) through the mid-thermocline (200–450 m layer) at the central mooring may be estimated using Pollard's calculation as  $F = \frac{1}{2}\rho(v_{\text{initial}}^2 - v_{\text{final}}^2)DT^{-1}$  where  $D = 250 \text{ m}$  is the thickness of the layer bounded above and below by current meters *C*<sub>1</sub> and *C*<sub>2</sub>, and  $T = 5 \text{ days}$  is the wake *e*-folding time scale. With initial and final layer ve-

locities of 20 and 7  $\text{cm s}^{-1}$  (from Fig. 8),  $F = 10 \text{ ergs cm}^{-2} \text{ s}^{-1}$ , which is about three times the Site D value. The vertical energy flux through the 200–450 m layer due to wave dispersion is  $F = C_{gz} \cdot E_d$ , where the layer kinetic energy density (*E*<sub>*d*</sub>) at the time of maximum wave response may be estimated as  $E_d = \frac{1}{2}\rho v^2 \approx 200 \text{ ergs cm}^{-3}$ . With  $C_{gz} = 60 \text{ m day}^{-1}$ , then  $F = 14 \text{ ergs cm}^{-2} \text{ s}^{-1}$ , consistent with the direct estimate.

The simple calculation given here does not consider horizontal energy fluxes in the local layer energy budget. However, it does provide an upper bound on the vertical energy flux required to account for the

TABLE 2. Comparison of inertial-internal wave parameters estimated from observations and predicted by a hurricane-response model.

	Hurricane Allen	Price (1983) model	Pollard (1980) "Site D"
Length scales			
Horizontal (km)	370	480	700–1700
Vertical (m)	1000	1000	100–240
Energy transport velocity			
Horizontal ( $\text{km day}^{-1}$ )	23	86	0.8–17
Vertical ( $\text{m day}^{-1}$ )	60	100	0.03–3
Energy travel time (days)			
50 km horizontally	2.2	0.6	63–3
100 km vertically	1.7	1.0	3000–30

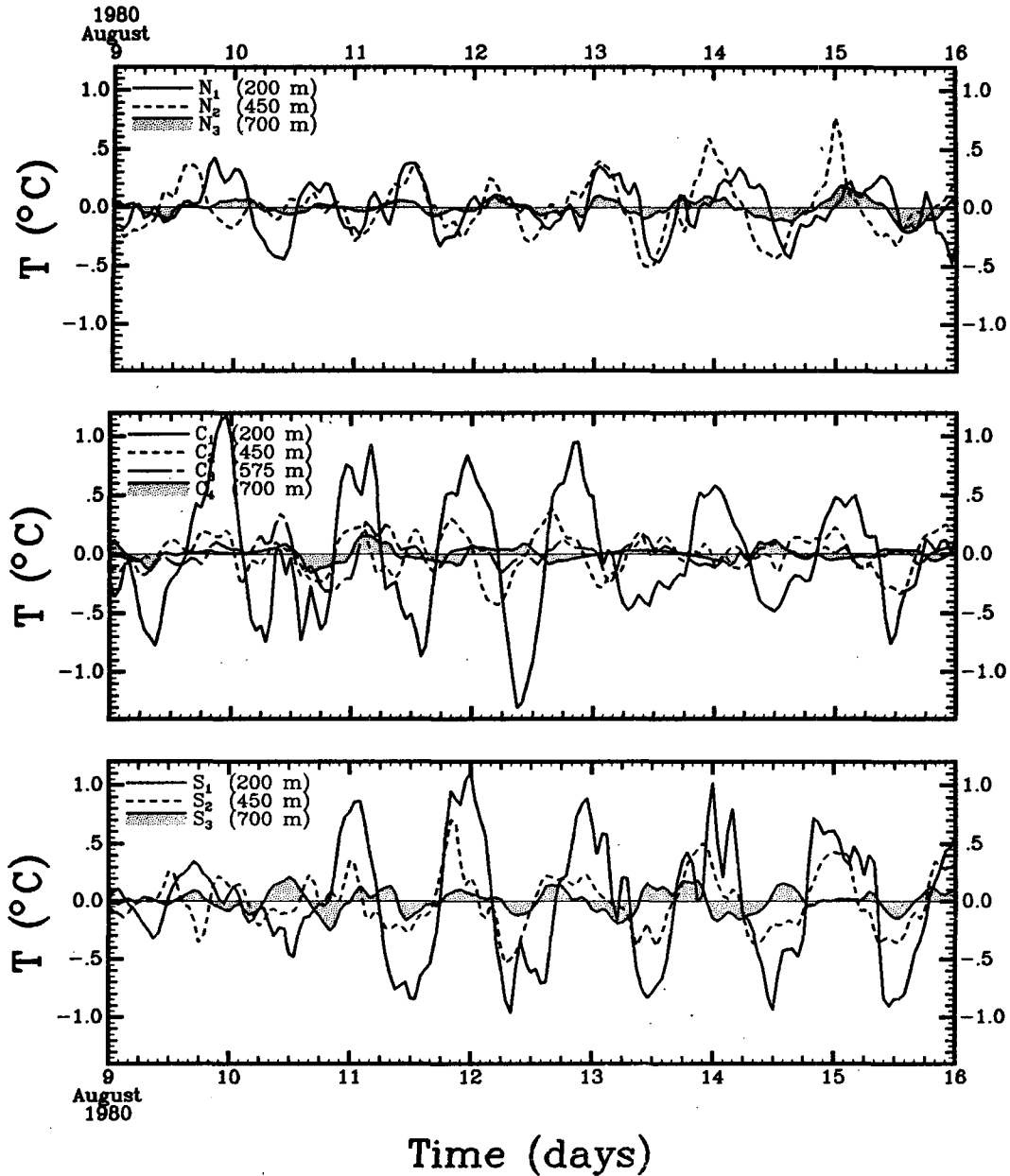


FIG. 10. Band-pass filtered temperature oscillations in the hurricane wake at the three moorings. These records show the buildup of leading phases with depth, and the decrease of amplitude away from the storm track.

observed depletion of kinetic energy in the thermocline. In contrast with the Site D case, the present analysis suggests that vertical energy dispersion in Hurricane Allen's wake was sufficient to account for the gross changes in mid-thermocline kinetic energy.

The present estimates of horizontal and vertical energy transport velocity are compared with Pollard's and with some model predictions by Price (1983) in Table 2. The Hurricane Allen estimates indicate the maximum wake response at the central mooring should have occurred several days after the closest passage of the storm's strongest winds, which is con-

sistent with Fig. 8. The round-trip time of energy transport between  $C_1$  (200 m depth) and the shelf edge,  $\sim 12$  km distant (Fig. 5b), is about 1 day, which suggests that reflection from the steep slope may have distorted the vertical phase distribution after 4 IP in Fig. 9. Bottom reflections may have had a similar effect.

The depth-leading phase of the wake is also apparent in the temperature, shown in Fig. 10 for all the instruments. The temperature oscillations can be interpreted as equivalent vertical displacement oscillations, or upwelling, with maximum displacements

of  $\sim \pm 20$  m (Appendix). In contrast with the long-shore current response, which was most intense at the central mooring, the temperature (upwelling) response had similar amplitudes at the southern and central moorings. The response at the northern mooring was relatively small.

The off-track  $v$ -component extended into the mid-thermocline, but not to the bottom (Fig. 11). Recent hurricane response models (Price, 1981, 1983) predict an asymmetry of the oceanic velocity, with the maximum displaced several storm radii to the right of the storm track. The same models predict cross-track symmetry of upwelling, with the maximum occurring on the track. Both of these tendencies are indicated in the vertical-plane contours of Fig. 11. However, Price's model hurricane was symmetric with a single wind speed maximum, showing that the asymmetry of the velocity response was a feature of the model ocean and not imposed by the forcing. Hurricane Allen's wind speed distribution was asymmetric with two wind speed maxima (Fig. 3). Thus, the off-track maximum of the observed storm response cannot be taken as unambiguous support of the model prediction. Also, the presence of the locally steep slope of the continental margin may have resulted in some channeling of the flow at the central mooring.

Contours of the displacement field at the central mooring thermistor string are shown as a function of depth and time in Fig. 12. The depth range spans the central third of the main thermocline, and the time axis spans the build-up phase of the wake response. The displacement contours show the rapid build-up of vertically coherent oscillations in the mid-thermocline. The first half-cycle after the storm passed (0000 GMT 10 August) consisted of an in-phase upwelling tendency in the thermocline, with positive displacements (shaded areas) between 240 and 290 m. The initial displacement period of about 0.5 IP lengthened to about 0.9 IP after one oscillation. By the time of the maximum wake response, approximately 3 IP after the storm passed, the displacement was nearly symmetric between  $\pm 20$  m, and it extended throughout the depth range spanned by the thermistor string (200–300 m). The small tilt of the isopleths indicates leading phases at depth, associated with downward energy propagation through the mid-thermocline. The large vertical scale of the displacement field is a central prediction of Price's model. The displacement amplitude was relatively uniform and highly coherent over the 100 m thick layer, also consistent with the model predictions. The displacement amplitude and vertical coherence decreased after 14 August, during the wake decay period.

**5. Summary and conclusions**

Hurricane Allen passed over an array of current meters moored over the 732 m isobath on the con-

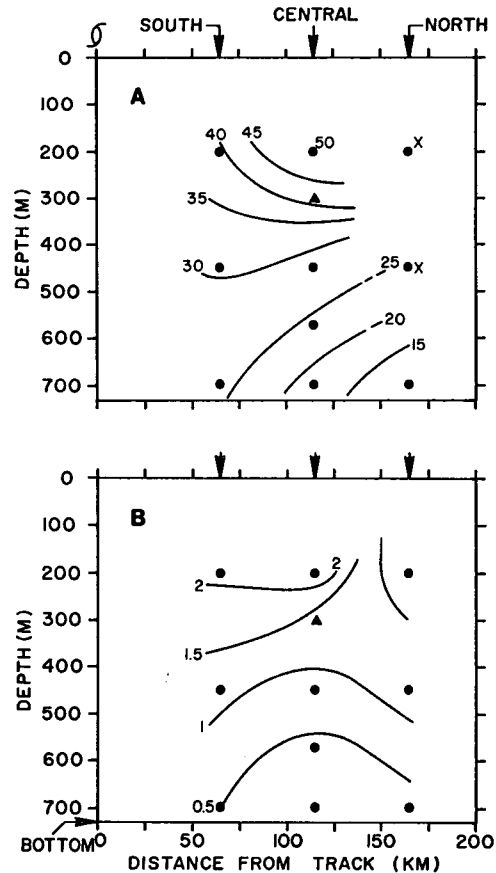


FIG. 11. Contours of the maximum  $v$ -component range [ $\text{cm s}^{-1}$ (A)] and maximum temperature range [ $^{\circ}\text{C}$ (B)] in the Hurricane Allen wake. The rotors were lost on the upper two current meters at the northern mooring so speed information was not available there. The velocity, but not the temperature, shows an off-track maximum.

tinental margin of the western Gulf of Mexico. The oceanic response to the storm consisted of a southward surge reaching  $91 \text{ cm s}^{-1}$  in the thermocline, with superimposed near-inertial wake oscillations growing to  $\sim 50 \text{ cm s}^{-1}$  about 3 days after the storm's passage. Thereafter, the wake amplitude diminished with a time scale of about 5 days, but residual effects of the disturbance lasted for many weeks.

The southward surge began under the southwestward wind stress of the approaching storm and lasted for about one day. The surge amplitude may have been intensified by the channeling effects of a local scarp-like feature, which was located about 12 km west of the array.

The near-inertial wake oscillations commenced as the eye of the storm passed. The period of the fully-developed wake was 22–23 h, or about 85% of the local inertial period (IP).

The early part (1–2 IP) of the wake response was nearly in-phase vertically, indicating a very large vertical length scale in the thermocline. By the time of

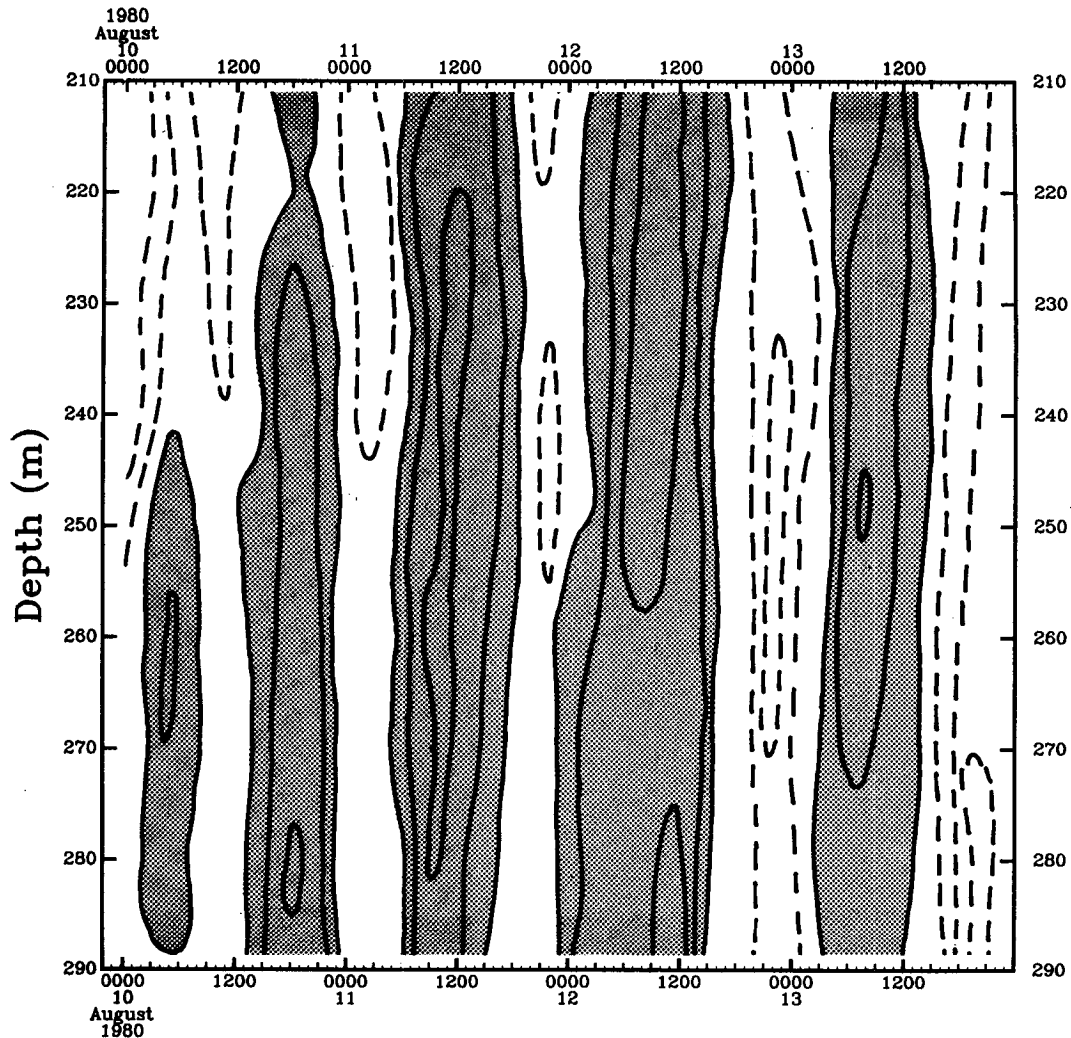


FIG. 12. Contours of vertical displacement (m) at the central mooring, for the depth range of the thermistor string (200–300 m) and the buildup phase of the wake oscillations (10–14 August). Regions of positive (upward) displacement relative to the background are shaded, and negative contours are dashed. The contour interval is 10 m.

the most energetic wake response ( $\sim 3$  IP), the phase lead of the velocity and temperature oscillations clearly increased with depth, indicating downward radiation of energy. The maximum phase difference between the current oscillations at the 200 and 575 m depths was about one-third cycle, indicating that the vertical scale in the thermocline was  $\sim 1$  km, still larger than the ocean depth. The large vertical scale of the wake results in an estimate of the vertical energy transport velocity of  $\sim 60$  m day $^{-1}$ , which provides a radiation energy flux sufficient to account for the observed depletion of the mid-thermocline wake kinetic energy. Energy reflection from the shelf edge or the bottom may have distorted the wake after about 4 IP.

Some of the features of the Hurricane Allen wake are consistent with recent hurricane response model

predictions (Price, 1983). The large vertical scale of the wake, especially during its inception, supports Price's result that the initial wake response consists of vertically near-uniform upwelling in response to a surface mixed-layer divergence. The model indicates that, after a few IP, thermocline mass field adjustments result in leading phases with depth, but that the vertical length scale remains large compared to the thermocline thickness scale. The Allen observations show a build-up of leading phases at depth, although the vertical scale (and hence the vertical energy transport rate) evidently remained large enough to radiate away the mid-thermocline wake kinetic energy.

*Acknowledgments.* The Hurricane Allen data were obtained during a study of the circulation in the west-

ern Gulf of Mexico, which was supported by the National Science Foundation under Grant OCE 79-24606. I thank M. Cooke, P. Blankinship, M. Ignaszewski and R. Cohen for their help with instrument and mooring preparations, the captains and crews of R/V *Gyre* and R/V *Columbus Iselin* for at-sea services, and T. Reid and M. Eblé for their data processing assistance. F. Kling painstakingly typed the manuscript. The wind speed data shown in Fig. 3 were provided by P. Black.

APPENDIX

Upwelling Inferred from Temperature

A scaling argument shows that the wake temperature oscillations in Figs. 7 and 10 can be interpreted as mostly due to vertical displacement of isotherms. Assuming a linear heat conservation equation for the thermocline region, i.e.,  $dT/dt = 0$ , it follows that

$$w' = -\left(\frac{\partial T'}{\partial t} + u \frac{\partial \bar{T}}{\partial x} + v \frac{\partial \bar{T}}{\partial y}\right)\left(\frac{\partial \bar{T}}{\partial z}\right)^{-1}, \quad (A1)$$

where overbars denote mean values and primes denote departures from the corresponding mean. The gradients of the mean temperatures ( $\partial \bar{T}/\partial y$ ,  $\partial \bar{T}/\partial z$ ) are approximately  $(10^{-5}, 10^{-2})^\circ\text{C m}^{-1}$ , as may be verified from Table 1 for the 29-day period centered on the storm. A near-inertial model is assumed for the wake, such that  $v' = V_0 \cos \omega t$ ,  $u' = U_0 \sin \omega t$  and  $T' = T_0 \sin \omega t$ ; here  $\omega = (2\pi/P)$ ,  $P \approx 22$  h is the wake period, and  $V_0$ ,  $U_0$ ,  $T_0$  are amplitude factors that vary on a time scale  $\gg P$ . From Fig. 7, appropriate choices at  $C_1$  are  $(V_0, U_0) = (0.25, 0.15) \text{ m s}^{-1}$  and  $T_0 = 1^\circ\text{C}$ . An estimate of  $\partial \bar{T}/\partial x$  is not available from the moored instruments, but it can be argued that  $\partial \bar{T}/\partial x \ll \partial \bar{T}/\partial y$  in the experiment area, based on Fig. 1 and on historical hydrographic data (e.g., Brooks and Eblé, 1982). Taking the equality as the largest expected estimate of  $\partial \bar{T}/\partial x$ , the terms in (A1) have the following orders of magnitude:

$$w' \sim O[0.8 \times 10^{-4}, 0.4 \times 10^{-5}, 0.4 \times 10^{-5}] [10^2] \text{ m s}^{-1}.$$

The mean velocities at the  $C_1$  instrument ( $\bar{u}_1$ ,  $\bar{v}_1$ ) have been added to the appropriate amplitude factors ( $U_0$ ,  $V_0$ ) in order to include an estimate of mean advection in the velocity terms ( $\bar{u} + U_0$ ,  $\bar{v} + V_0$ ) of (A1).

With these scale estimates, the perturbation tem-

perature in the mid-thermocline may be reasonably converted to vertical isotherm displacement as

$$\eta' = \int w' dt \approx -T' \left(\frac{\partial \bar{T}}{\partial z}\right)^{-1}. \quad (A2)$$

It is understood that the wake perturbations (primed quantities) occur with respect to a slowly-varying "mean" field which has time scales much longer than the inertial period. Thus, the calculation in (A2) was done using the 3–40 h band-passed data for  $T'$  and the 40 h low-passed data for  $\partial \bar{T}/\partial z$ . The maximum amplitude of  $\eta'$  calculated from (A2) is about 20 m in the mid-thermocline, in reasonable agreement with Price's (1983) model predictions.

REFERENCES

Brooks, D. A., and M. C. Eblé, 1982: Hydrographic observations in the western Gulf of Mexico. Data Report, R/V *Gyre* Cruises 80-G-1, 80-G-11, 81-G-1; R/V *Columbus Iselin* Cruise I-80-06. Texas A&M University Ref. 82-2-T, 174 pp.

—, and R. V. Legeckis, 1982: A ship and satellite view of hydrographic features in the western Gulf of Mexico. *J. Geophys. Res.*, **87**, 4195–4206.

Forristall, G. Z., R. C. Hamilton and V. J. Cardone, 1977: Continental shelf currents in tropical storm Delia: Observations and theory. *J. Phys. Oceanogr.*, **7**, 532–546.

Franceschini, G. A., and S. Z. El-Sayed, 1968: Effect of Hurricane Inez (1966) on the hydrography and productivity in the Western Gulf of Mexico. *Sonderdruck Dtsch. Hydrogr. Z.*, **21**, No. 5.

Jones, W. L., P. G. Black, V. E. Delnore and C. T. Swift, 1981: Airborne microwave remote-sensing measurements of Hurricane Allen. *Science*, **214**, 274–280.

Merrell, W. J., and J. M. Morrison, 1981: The current regime of the western Gulf of Mexico as observed in April 1978. *J. Geophys. Res.*, **86**, 4181–4186.

Nowlin, W. D., Jr., 1972: Winter circulation patterns and property distributions. *Contributions on the Physical Oceanography of the Gulf of Mexico*, L. Capurro and J. Reid, Eds., Gulf Publ., pp. 3–51.

Phillips, O. M., 1969: *The Dynamics of the Upper Ocean*. Cambridge University Press, 261 pp.

Pollard, R. T., 1980: Properties of near-surface inertial oscillations. *J. Phys. Oceanogr.*, **10**, 385–398.

Price, J. F., 1981: Upper ocean response to a hurricane. *J. Phys. Oceanogr.*, **11**, 153–175.

—, 1983: Internal wave wake of a moving storm. Part I: Scales, energy budget and observations. Submitted to *J. Phys. Oceanogr.*

Smith, N. P., 1978. Longshore currents on the fringe of Hurricane Anita. *J. Geophys. Res.*, **83**, 6047–6051.

Woodley, J. D., E. A. Chornesky, P. A. Clifford, J. B. C. Jackson, L. S. Kaufman, N. Knowlton, J. C. Lang, M. P. Pearson, J. W. Porter, M. C. Rooney, K. W. Rylaarsdam, V. J. Tunnicliffe, C. M. Wahle, J. L. Wulff, A. S. G. Curtis, M. D. Dallmeyer, B. P. Jupp, M. A. R. Koehl, J. Neigel and E. M. Sides, 1981: Hurricane Allen's impact on Jamaican coral reefs. *Science*, **214**, 749–755.